External Filtered Modes of a Quantum Dot Laser Under the Influence of Double-Filtered Optical Feedback

Alaa S. Mahdi[1],Hussein B. Al Husseini[1, 2]

[1] *Department of Physics, College of Sciences, University of Thi-Qar, Iraq; E-mail: Alaa_sal.ph@sci.utq.edu.iq*

[2] *College of Education, Al-Ayen University, Thi-Qar, 64001, Iraq; E-mail: drhussain@sci.utq.edu.iq*

Abstract: When semiconductor lasers SLs are exposed to filtered optical feedback (FOB), they behave in two different ways. Under weak or strong feedback, the first is a singularly stable longitudinal mode with a small linewidth. The second is the so-called coherence breakdown condition, which also includes low frequency fluctuations (LFF) and chaotic oscillations. The latter has received a lot of attention recently due to the possible uses of chaotic lasers in chaotic lidar, covert communications, and chaotic correlation time-domain optical reflectometers, while the former has received a lot of research in recent years. We investigate the behavior of a quantum dot (QD) semiconductor laser subject to FOF from two separate external cavities both, numerically and experimentally. Our findings show that the second FOF allows for rich adjustment of the laser frequency. Our analysis of double-filtered optical feedback (DFOF) lasers is on fundamental solutions, sometimes referred to as continuous waves (CW) or external filtering modes (EFM), which result in a QD laser output with constant amplitude and frequency. The time delay suppression is dependent on the spectral width Λ of the filter and how far it is from the solitary laser frequency, according to numerical calculations.

Keywords: Quantum Dot Laser, External Filtered Mods, Double-Filtered Optical Feedback.

1. Introduction

The nonlinear response to perturbations, which manifests in pronounced sensitivity to things like external optical injection, variations in injection current, noise, or delayed optical feedback, is a distinguishing characteristic of the majority of SLs. This apparent sensitivity is particularly intriguing because even small amounts of reinjected light can cause chaotic dynamics and disrupt SL emission. For applications needing steady emission, even a tiny back reflection from the end of an optical fibre can cause the SL to become unstable [1-3].

The laser with feedback from an external cavity is known to show a wide range of dynamics . Unfortunately, the dynamics are controlled by a relatively small number of potentially unreachable control factors, necessitating painstaking accuracy in the analysis . Recently, we suggested using a frequency filter in the external cavity to regulate a variety of feedback light characteristics and therefore affect the feedback system . To change the feedback light and achieve the appropriate dynamics, the filter's two additional control parameters, including its spectral bandwidth and the location of its central frequency in relation to the single (stand-alone) laser frequency, can be used to alter the feedback light such that desired dynamics may be achieved[4, 5] .

The dynamical response of the laser must be controlled with reliable procedures in order to profitably use the dynamics in the right devices. We have demonstrated in previous studies that filtered optical feedback (FOF), in which the feedback is spectrally filtered before being transmitted back into the laser, is one potential possibility for exerting this control. Of course, spectrum filtering of feedback light into semiconductor lasers is frequently observed in some applications where the dynamics of the laser are unimportant. One typical technique for getting a semiconductor laser to operate in single mode is to use feedback from a diffraction grating. In these circumstances, the laser is fed back a particular spectral component of the diffracted light,and hence this forms a good example of utilizing filtered feedback[6, 7].

According to the ratio of the filter bandwidth Λ, the inverse of the external cavity roundtrip time τ^{-1} , and the relaxation oscillations (RO) frequency vRO, the filtered feedback may generally be divided into three distinct regimes . The feedback light will be (nearly) unaffected by the filter if Λ is greater than RO, and the system will exhibit typical conventional optical feedback (COF) dynamics. The system will be in the filtered feedback (FOF) regime if Λ is smaller

than RO but larger than τ^{-1} . In this case, the dynamics may be very different from the comparable COF dynamics. Finally, the dynamics will primarily be controlled by the filter if Λ is smaller than both RO and τ^{-1} [8].

The Lange-Kobayashi approach applied to a standard QD laser model is used to investigate the sensitivity of quantum dot SLs to optical feedback. Right now, this trait is a fascinating subject. These materials' discrete energy transitions lead to symmetrical emission lines and consequently a low factor. This led to stimulated numerous research projects, with anticipated benefits including the elimination of chirp in high-speed applications, lasers insensitive to optical feedback, and broadband devices that operate without filaments. Optical isolators are necessary in many applications due to the extreme sensitivity of bulk and quantum-well semiconductor lasers to back reflections. Given these conditions, numerous dynamic behaviors are possible. [9].

Normally, in an SL based system, nonlinearities are not expected due to the quick intra-band relaxation rate but can be achieved by introducing some external effects, such as;

1- Injection of external optical signals [10].

2-Modulation of pumping currents[11].

3-Feedback through an external cavity [12].

Quantum Dot laser model with DFOF

Any frequency and filter width combination can be scanned for on the system. Finally, this type of experimental setup with a single FOF loop has been successfully used in single laser FOF studies [13]. Particularly, it has been demonstrated that a rate equation model, in which the filters are anticipated to have a Lorentzian transmittance profile, provides a very good representation of the system [14, 15]. The following rate equations can be used to describe the system:

$$E^{\bullet} = -\frac{1}{2}\gamma_s E + \frac{1}{2}(1+i\alpha)vg_o\left(2\rho_{gs}-1\right)E + \frac{k_1}{2}F_1(t) + \frac{k_2}{2}F_2(t) \quad (1)$$

$$F_1^{\bullet} = \Lambda_1\, E_{\tau 1}e^{-i\theta} + (i\omega_{m1} - \Lambda_1\,)F_1(t) \qquad (2)$$

$$F_2^{\bullet} = \Lambda_2\, E_{\tau 2}e^{-i\theta} + (i\omega_{m2} - \Lambda_2\,)F_2(t) \qquad (3)$$

with normalized feedback strengths k_1 and k_2 of the normalized filter fields $F_1(t)$ and $F_2(t)$, the two FOF loops enter as feedback terms $k_1F_1(t)$ and $k_2F_2(t)$ In Eq . (1). The quantity Θ is a key parameter because it governs the effective feedback strength by influencing interference between the two filter fields [16]. Generally, the filter's inclusion in the system results in an integral equation for the filter field. Where first and second loop round-trip times are τ_1 and τ_2, respectively.

By sub $F_1(t) = F_{C1}(t) + iF_{S1}(t)$ and $F_2(t) = F_{C2}(t) + iF_{S2}(t)$ in Eq (2) and (3) We will get

$$S^{\bullet} = \left[vg_o\left(2\rho_{gs}-1\right) - \gamma_s\right]S + k_1F_{c1} + k_1F_{c1} \qquad 4(a)$$

$$\varphi^{\bullet} = \frac{-\alpha}{2}vg_o\left(2\rho_{gs}-1\right) - \frac{k_1}{2}\,F_{S1} - \frac{k_2}{2}\,F_{S2} \qquad 4(b)$$

$$F_{C1}^{\bullet} = 2\Lambda_1\sqrt{SS_{\tau 1}}\;cos(\varphi + \varphi_{\tau 1} + \Theta) - \omega_{m1}F_{s1} - \Lambda_1F_{c1} \qquad 4(c)$$

$$F_{s1}^{\bullet} = -\Lambda_1 \sqrt{\frac{S_{\tau 1}}{S}}\, sin(\varphi + \varphi_{\tau 1} + \Theta) + \omega_{m1} F_{c1} - \Lambda_1 F_{s1} \qquad 4(d)$$

$$F_{C2}^{\bullet} = 2\Lambda_2 \sqrt{S S_{\tau 2}}\, cos(\varphi + \varphi_{\tau 2} + \Theta) - \omega_{m2} F_{s2} - \Lambda_2 F_{c2} \qquad 4(c)$$

$$F_{s2}^{\bullet} = -\Lambda_2 \sqrt{\frac{S_{\tau 2}}{S}}\, sin(\varphi + \varphi_{\tau 2} + \Theta) + \omega_{m2} F_{c2} - \Lambda_2 F_{s2} \qquad 4(d)$$

The carrier-light interaction in our approach is summarized in (S), which contains longitudinal modes. Our model, which is used in this study, is a modified version of the Al-Husseini model for optical feedback in QD lasers [17], in which the PCM provides feedback through the external cavity to a single-mode QD semiconductor laser. τ and k are crucial factors in any optical feedback system. Additionally, DFOF is a form of coherent feedback, which means that the phase difference between the outgoing and returning light is also an important factor. Optical feedback can be used in a variety of applications, including optical communications and optical recording. Back reflections from lenses, optical fibers, or surfaces can affect the laser's status. Because semiconductor lasers are open, optical light can enter more freely. Different dynamical regimes can emerge as a result of this feedback. Low Frequency Fluctuations are one of the regimes that occur for injection currents near the threshold [18].

The spectral widths Λ_1 and Λ_2 and the detuning of the filters' central frequencies ω_{m1} and ω_{m2} from the solitary laser frequency are used to determine the filters' optical properties. both relations of the DFOF laser can be modeled by the dimensionless: The authors added new variables to this step.

$\eta_1 = \frac{k_1}{\gamma_s}$, $\eta_2 = \frac{k_2}{\gamma_s}$, $\Omega_{m1} = \frac{\omega_{m1}}{\gamma_s}$, $\Omega_{m2} = \frac{\omega_{m2}}{\gamma_s}$

$$x^{\bullet} = x\,(y-1) + \eta_1 \frac{\Gamma_1}{\Gamma_2} F_{c1} + \eta_2 \frac{\Gamma_1}{\Gamma_2} F_{c2} \qquad 5(a)$$

$$\varphi^{\bullet} = \frac{-\alpha}{2} y - \frac{1}{2}\eta_1 F_{S1} - \frac{1}{2}\eta_2 F_{S2} \qquad 5(b)$$

$$F_{C1}^{\bullet} = 2\ \lambda_1\, \Gamma_2/\Gamma_1 \sqrt{x x_\tau}\, cos(\varphi + \varphi_\tau + \Theta) - \Omega_{m1} F_{s1} - \lambda_1 F_{c1} \qquad 5(c)$$

$$F_{s1}^{\bullet} = -\lambda_1 \sqrt{\frac{x}{x_\tau}}\, sin(\varphi + \varphi_\tau + \Theta) + \Omega_{m1} F_{c1} - \lambda_1 F_{s1} \qquad 5(d)$$

$$F_{C2}^{\bullet} = 2\ \lambda_2\, \Gamma_2/\Gamma_1 \sqrt{x x_\tau}\, cos(\varphi + \varphi_\tau + \Theta) - \Omega_{m2} F_{s2} - \lambda_2 F_{c2} \qquad 5(c)$$

$$F_{s2}^{\bullet} = -\lambda_2 \sqrt{\frac{x}{x_\tau}}\, sin(\varphi + \varphi_\tau + \Theta) + \Omega_{m2} F_{c2} - \lambda_2 F_{s2} \qquad 5(d)$$

changing the length of the feedback loop on the nanometer optical wavelength scale changes Θ, but τ does not effectively change, as has been experimentally justified. Experimentally, has been altered using two separate methods [15, 19]: in [19], a piezo actuator is used to change the feedback loop's length on an optical wavelength scale, and in [15] Θ is modified indirectly by extremely slight variations in the pump current, which in turn impact ω_O. The structure of the fundamental continuous wave (CW) solutions, commonly known as external filter modes (EFM), is greatly affects by the addition of the second filter [20].

External filtered modes of DFOF

A laser that generates monochromatic light with specified amplitude and a defined frequency ω_s (relative to the solitary laser frequencyω_0) is the most basic non-zero solution for a DFOF laser. These are EFMS solutions. Mathematically, the EFM is the orbital of a group of Eqs. 5(a) - 5(d) under S^1 - symmetry, which means it takes the form[20].

$$E = E_s e^{i\omega_s t} \ , F_1 = F_{s\ s}^1 e^{i(\omega_s t+\varphi_1)} \ , F_2 = F_{s\ s}^2 e^{i(\omega_s t+\varphi_2)} \ldots\ldots\ldots (6)$$

The phase shifts between the two filter fields and the laser field are φ_1 and φ_2. Due to the fact that the EFM surface's intersection curves with constant Θ planes are EFM components and are identical to those of a single FOF laser, it is a natural object for exploring fundamental solutions in a DFOF laser. In a nutshell, the EFM surface is a collection of all EFM elements that could be found in a DFOF laser for different, constant values of Θ. To find the EFMs we substitute Eq. (6) into Eqs. (1) - (3) and when we isolate the real and imaginary parts we get:

$$\omega_S = \frac{\alpha}{2}\gamma_s + \frac{k_1\Lambda_1\sqrt{1+\alpha^2}}{2\sqrt{\Lambda_1^2+(\omega_S - w_{M1})^2}} \sin(\varphi_1 - \tan^{-1}\alpha) + \frac{k_2\Lambda_2\sqrt{1+\alpha^2}}{2\sqrt{\Lambda_2^2+(\omega_S-\omega_{M2})^2}} \sin(\varphi_2 - \tan^{-1}\alpha) \qquad (7)$$

$$\Omega(\omega_s) - \omega_s = 0 \qquad (8)$$

$$\Omega(\omega_S) = \frac{\alpha}{2}\gamma_s + C_{eff1}\sin(\varphi_1 - \tan^{-1}\alpha) + C_{eff2}\sin(\varphi_2 - \tan^{-1}\alpha) \qquad (9)$$

Where

$$C_{eff1} = \frac{k_1\Lambda_1\sqrt{1+\alpha^2}}{2\sqrt{\Lambda_1^2+(\omega_S-\omega_{M1})^2}} \quad , \quad C_{eff2} = \frac{k_2\Lambda_2\sqrt{1+\alpha^2}}{2\sqrt{\Lambda_2^2+(\omega_S-\omega_{M2})^2}}$$

$$\varphi_1 = -\omega_S\tau_1 - \Theta - tan^{-1}(\frac{\omega_S-\omega_{M1}}{\Lambda_1})$$

$$\varphi_2 = -\omega_S\tau_2 - \Theta - tan^{-1}(\frac{\omega_S-\omega_{M2}}{\Lambda_2})$$

A specific set of filter parameters can be used to determine all possible EFM frequencies ω_S using equation (8), which is an implicit and transcendental equation. More specifically, by finding the root in Eq. (8), the required frequency values ω_S for the DFOF laser can be calculated numerically, for instance using Newton's technique with numerical continuity. The first and second terms in the sum of Eq. (9) represent, respectively, the first and second filters. For the frequency of the EFMs of the single FOF laser, Eq. (8) reduces to the transcendental equation in [21] if one of the k is set to zero. The remaining state variables have the following values.

$$F_s^1 = \frac{E_S\ \Lambda_1}{\sqrt{\Lambda_1^2+(\omega_S-\omega_{M1})^2}}$$

$$F_s^2 = \frac{E_S\ \Lambda_2}{\sqrt{\Lambda_2^2+(\omega_S-\omega_{M2})^2}}$$

$$Y_s = \frac{(1+2\alpha\Omega s)}{(\alpha^2+1)} \pm \sqrt{\frac{(1+2\alpha\Omega s)^2}{(\alpha^2+1)^2} - \frac{4\Omega_s^2+1}{(a^2+1)} - \frac{4\varsigma_1^2}{(a^2+1)\sqrt{1+(\frac{\omega_s-\omega_{m2}}{\Lambda_2})^2)}} - \frac{4\varsigma_2^2}{(a^2+1)\sqrt{1+(\frac{\omega_s-\omega_{m2}}{\Lambda_2})^2)}}}$$

Or

$$Y_s = C_O \pm \sqrt{C_O^2 - C_1 - \frac{4\,\eta_1^2}{(a^2+1)\sqrt{1+(\frac{\omega_s-\omega_{m2}}{\Lambda_2})^2)}} - \frac{4\eta_2^2}{(a^2+1)\sqrt{1+(\frac{\omega_s-\omega_{m2}}{\Lambda_2})^2)}}}$$

Where

$$C_O = \frac{(1+2\alpha\Omega s)}{(\alpha^2+1)} \quad , C_1 = \frac{4\Omega_S^2+1}{(a^2+1)} \quad , \eta_1^2 = \frac{\xi_1^2}{{\gamma_s}^2}, \quad \eta_2^2 = \frac{\xi_2^2}{{\gamma_s}^2}$$

The foundation for DFOF laser dynamics is the justification for the EFM surface categorization described in the preceding section. From this vantage point, understanding EFM devices is crucial even when they are of the saddle type, which is not stable. The dynamics of delayed feedback lasers can be significantly controlled by saddle-type continuous waves (CW), it has been demonstrated. The most well-known is the finding that the CW saddle of the COF lasers plays a significant role in frequent and irregular power outages known as low-frequency fluctuations and coherence breakdown. In more detail, saddle CWs are approached along their stable path as the laser power builds up, and only then is the trajectory reinjected along an unstable CW direction to an area of low power and the build-up process. [20].

EFMs of DFOF results

The special case, in which the two filters are identical, aside from having various feedback phases, serves as the beginning point for a study of the EFM structure. Hence, we now set $k_1 = k_2$ and $\tau_1 = \tau_2$. Figure 1 summarizes all the pertinent geometric information required to recognize and categorize EFMs. As also indicated, saddle-node bifurcations are where the EFMs are formed and lost. Although there is an important difference, this geometrical image is extremely similar to that of a single FOF laser. The envelope $\Omega(\omega_S)$ of the FOF laser is found by considering the extremes of the sine function (in Eq. (9), for example, $k_2 = 0$). It turns out that the fourth-order polynomial whose roots are the boundary points of at most two periods (or components) with potential EFMs can accurately describe the envelope of a single FOF laser [22]. However, for a DFOF laser, considering the extrema of the two sine functions in Eq. (9) is not enough because they exist in the total.

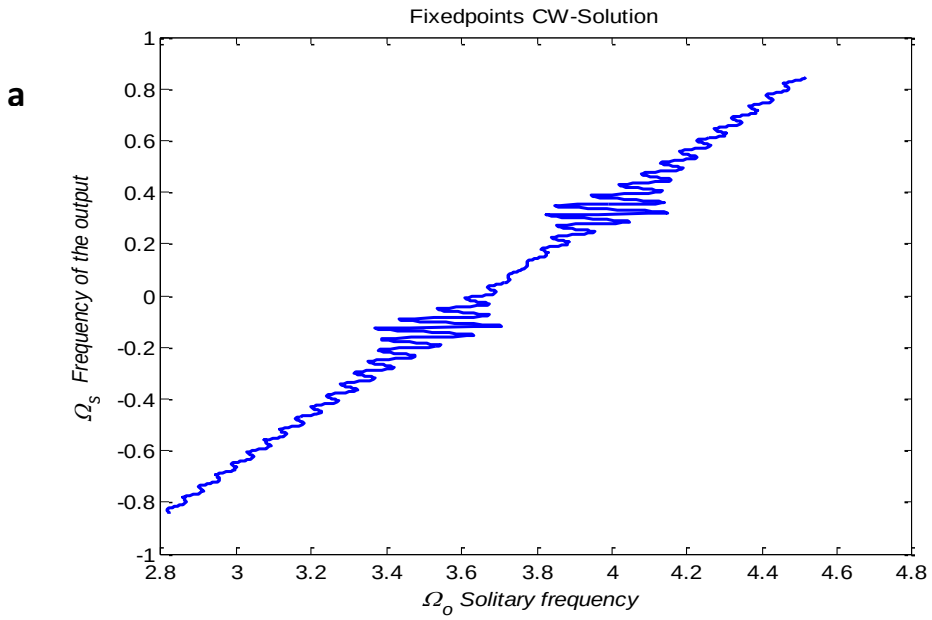

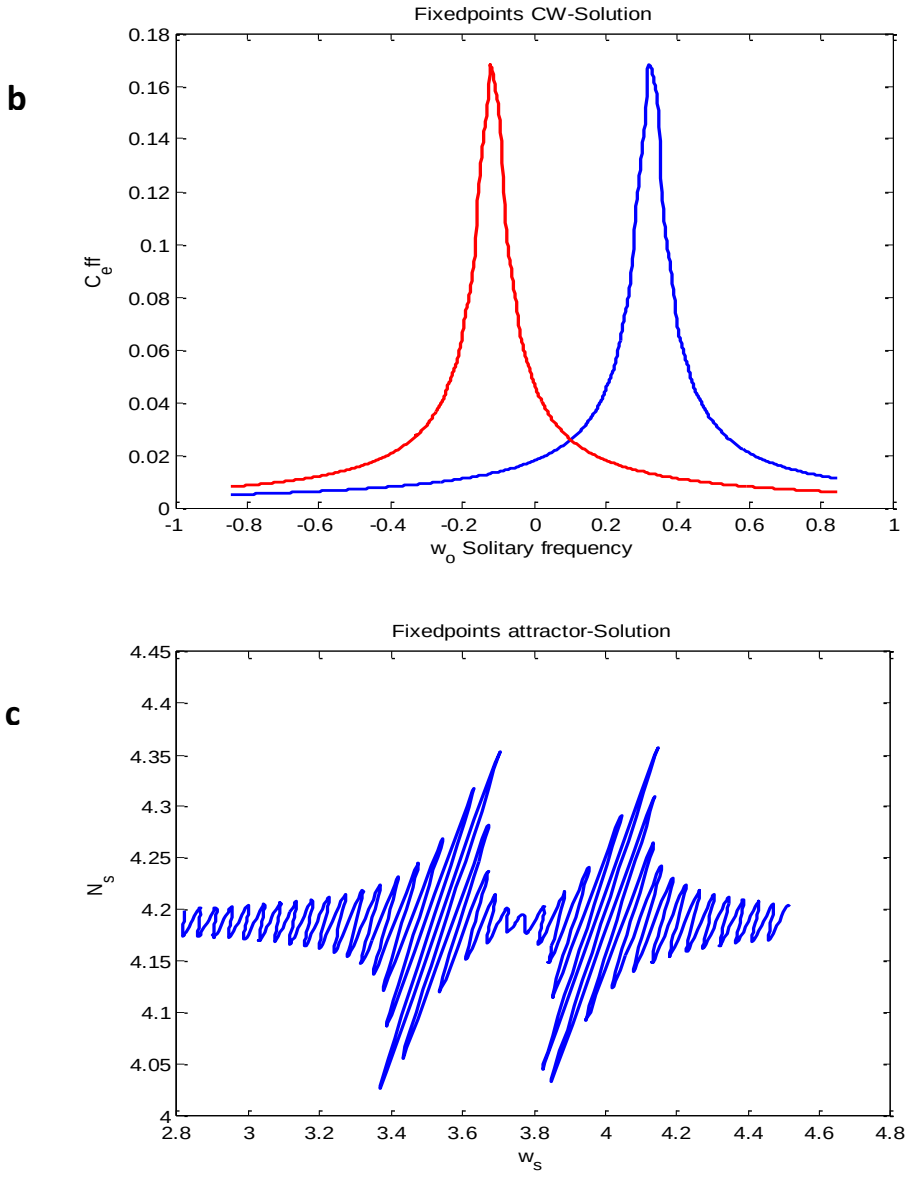

Fig.1: (a) (Ω_S, Ω_o) plane explained the fixed points on it at k_1 =k_2=0.25, $\tau_1 = \tau_2 = 3.8$ and $\omega_{f1} = 50/pi$, $\omega_{f2} = -2.5/pi$. (b) in (C_{eff}, Ω_o) plane projected the EFMs branches on it. The first and second filters are represented by blue and red curves respectively. With the appearance of the solitary QD-laser frequency is changed, the fixed points are established and ruined in CW-state bifurcations. (c) EFMs branches predictably addicted to the (N_S, ω_s) plane.

EFMs of DFOF under the influence of changing(ω_{f1}*and* ω_{f2})

When the value of ω_{f1} is changed to 20/pi while fixing the value of ω_{f2}, we notice from Fig.2(a) that the Lorentz profile for the first filter and the second filter converge to each other, and we notice this convergence clearly in Fig. 2(b) and 2(c).

In Fig. (3) we fix $\omega_{f1} = 50/pi$, and change ω_{f2} from $\omega_{f2} = -2.5/pi$, to $\omega_{f2} = -0.01/pi$ and $\omega_{f2} = 2.5/pi$, We note that this figure is completely identical to Fig. (1).

a

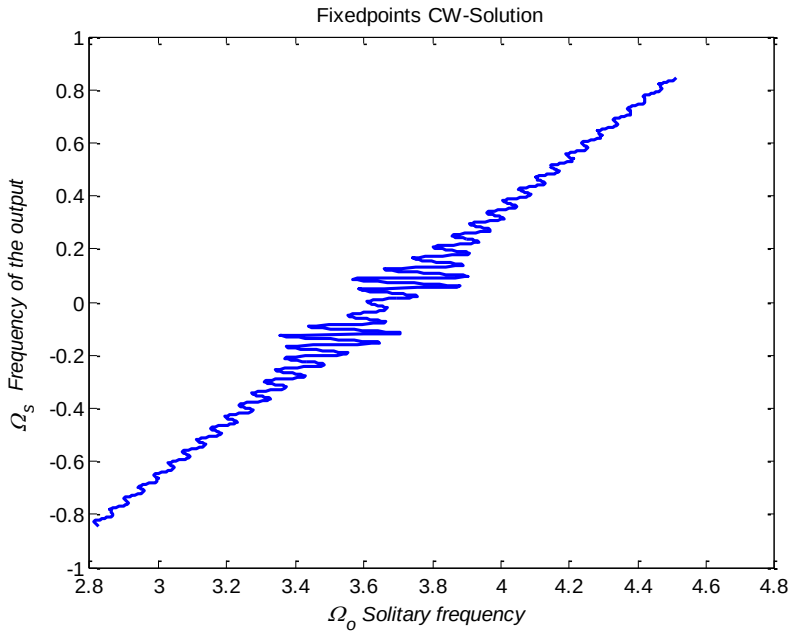
Fixedpoints CW-Solution
Ω_s Frequency of the output
Ω_o Solitary frequency
1
0.8
0.6
0.4
0.2
0
-0.2
-0.4
-0.6
-0.8
-1
2.8
3
3.2
3.4
3.6
3.8
4
4.2
4.4
4.6
4.8

b

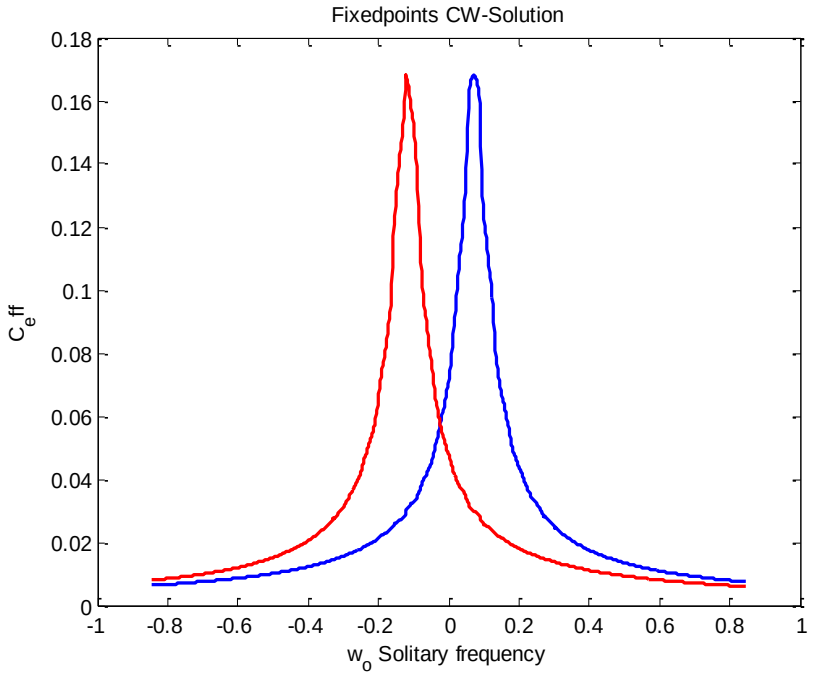
Fixedpoints CW-Solution
C_eff
w_0 Solitary frequency
0.18
0.16
0.14
0.12
0.1
0.08
0.06
0.04
0.02
0
-1
-0.8
-0.6
-0.4
-0.2
0
0.2
0.4
0.6
0.8
1

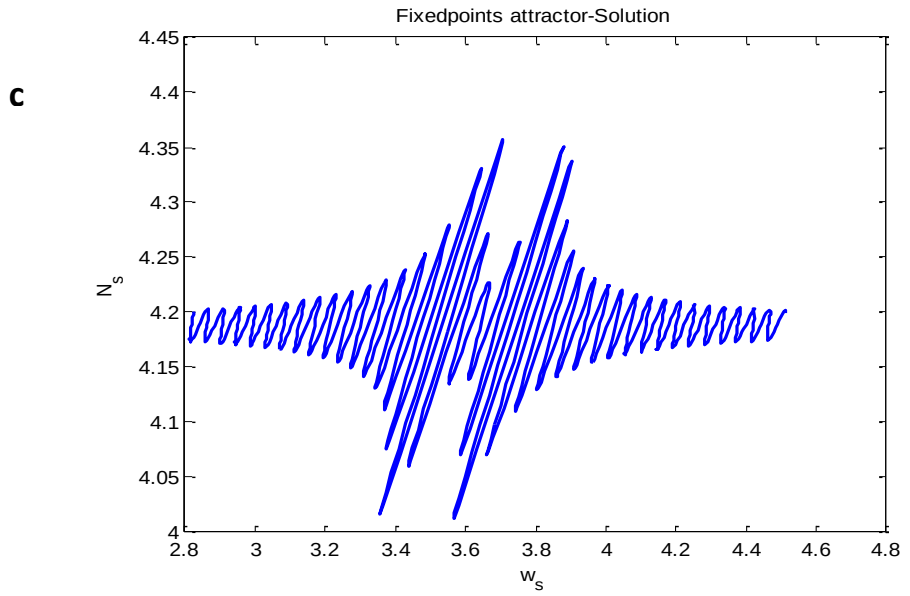

Fig.2: (a) (Ω_S, Ω_o) plane explained the fixed points on it at k_1 =k_2=0.25, $\tau_1 = \tau_2 = 3.8$ and $\omega_{f1} = 20/pi$, $\omega_{f2} = -2.5/pi$. (b) in (C_{eff}, Ω_o) plane projected the EFMs branches on it. The first and second filters are represented by blue and red curves respectively. With the appearance of the solitary QD-laser frequency is changed, the fixed points are established and ruined in CW-state bifurcations. (c) EFMs branches predictably addicted to the (N_S, ω_s) plane.

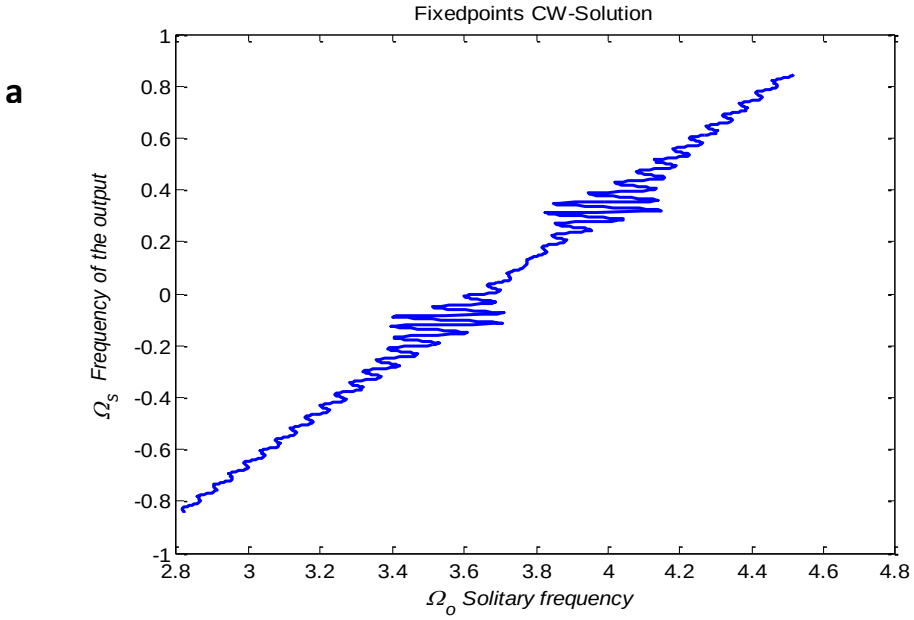

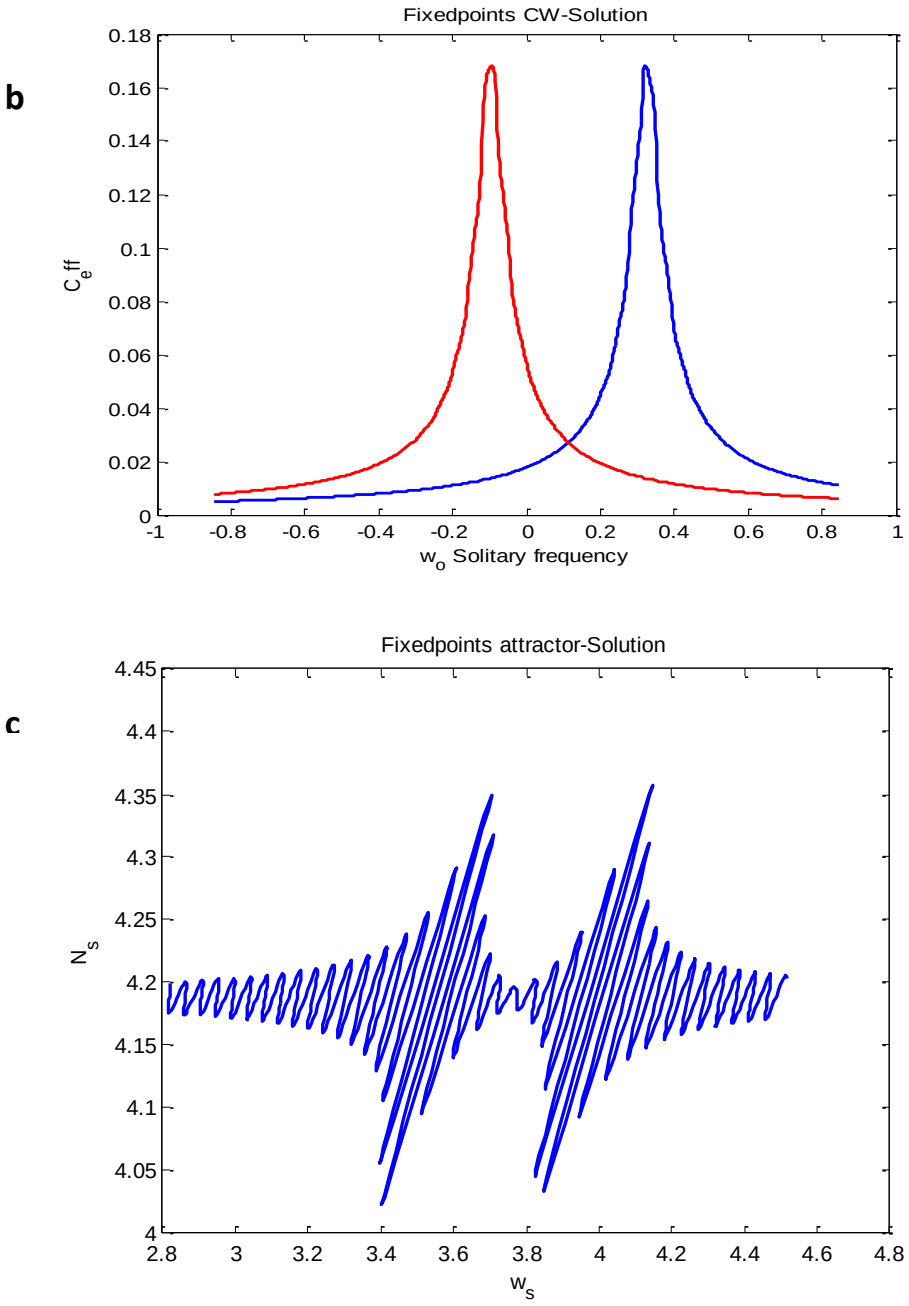

Fig.3: (a) (Ω_S, Ω_o) plane explained the fixed points on it at k_1 =k_2=0.25, $\tau_1 = \tau_2 = 3.8$ and $\omega_{f1} = 50/pi$, $\omega_{f2} = -0.01/pi$. (b) in (C_{eff}, Ω_o) plane projected the EFMs branches on it. The first and second filters are represented by blue and red curves respectively. With the appearance of the solitary QD-laser frequency is changed, the fixed points are established and ruined in CW-state bifurcations. (c) EFMs branches predictably addicted to the (N_S, ω_s) plane.

EFMs of DFOF under the influence of changing $(\tau_1 and\ \tau_2)$

When taking a large value for τ_1 , $\tau_1 = 7.132$, we notice an increase and clarity of the Lorentz profile for the first filter, as the width of the region extends from 3.7 to 4.2, as in Fig. 4(a). From Fig. 4(b), we notice that there is a distortion at the peak of the pulse for the first filter.

The wiggling shape is clear for the first filter compared to the wiggling shape for the second filter, in addition to the appearance of two clear saddle –nodes, as in Fig. 4(c). Fig. 4 shows us that any number of cavities can be found by taking large values of τ.

When the value of τ_2 changes from $\tau_2 = 3.8$ to $\tau_2 = 8$, this change leads to the clarity of the Lorentz profile for the second filter compared to the first filter, and this region extends from 3.3 to 3.7, as in Fig. 5(a).

From Fig. 5(b), we notice that there is a distortion at the peak of the second filter pulse. This distortion is within a period of 0.14.

Increasing τ_2 has a clear and significant effect on Fig. 5(c), where we notice the formation of three large and clear saddle nodes on the wiggling shape of the second filter, while the first filter maintains its wiggling shape without any saddle nodes.

a

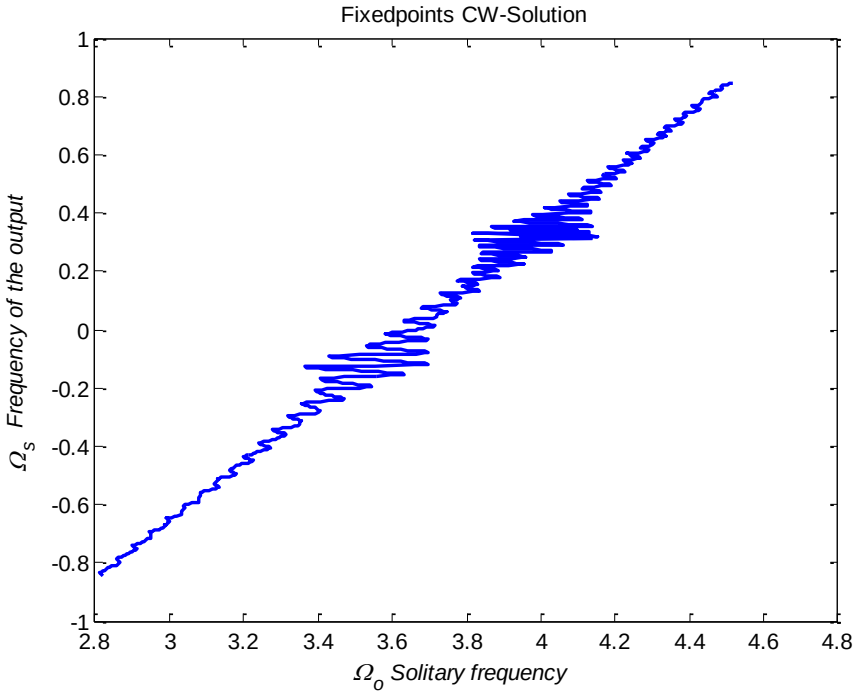

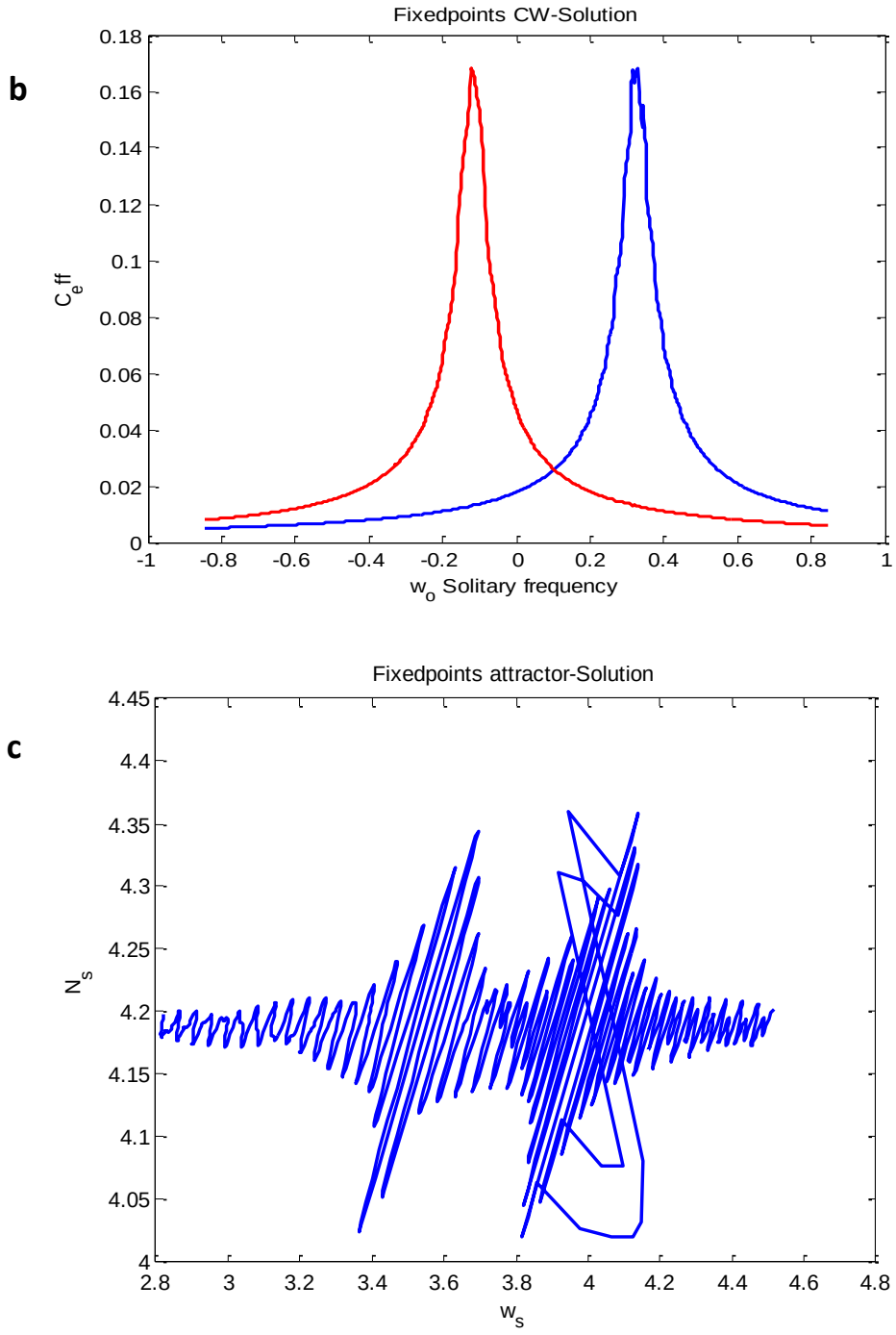

Fig.4: (a) (Ω_S, Ω_o) plane explained the fixed points on it at k_1 =k_2=0.25, $\tau_1 = 7.132$, $\tau_2 = 3.8$ and $\omega_{f1} = 50/pi$, $\omega_{f2} = -2.5/pi$. (b) in (C_{eff}, Ω_o) plane projected the EFMs branches on it. The first and second filters are represented by blue and red curves respectively. With the appearance of the solitary QD-laser frequency is changed, the fixed points are established and ruined in CW-state bifurcations. (c) EFMs branches predictably addicted to the (N_S, ω_s) plane.

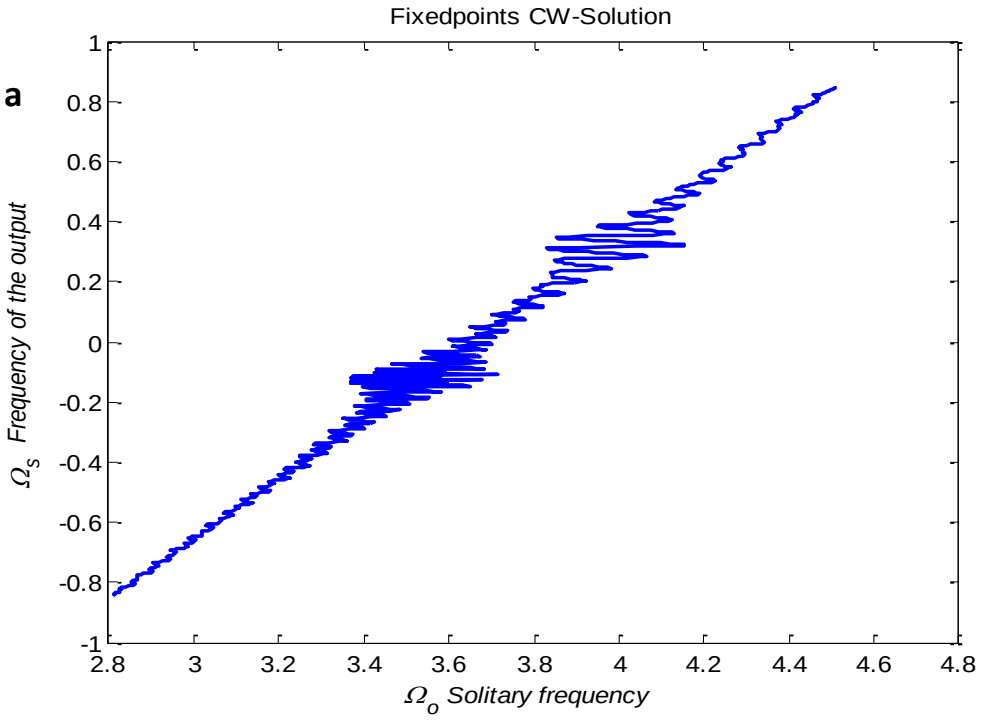
a
Fixedpoints CW-Solution
Ω_S Frequency of the output
Ω_o Solitary frequency
1
0.8
0.6
0.4
0.2
0
-0.2
-0.4
-0.6
-0.8
-1
2.8
3
3.2
3.4
3.6
3.8
4
4.2
4.4
4.6
4.8

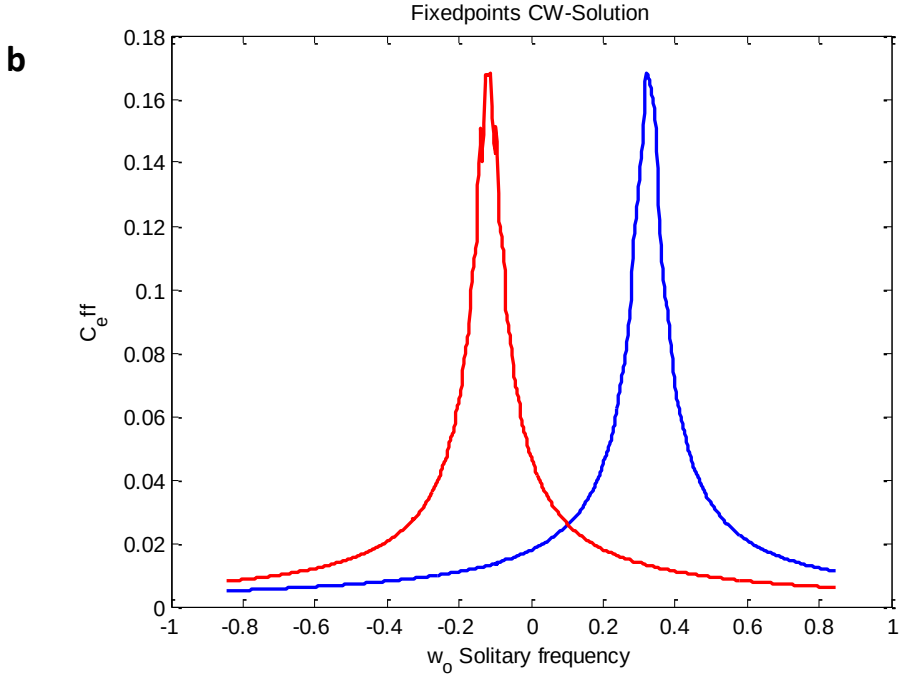
b
Fixedpoints CW-Solution
C eff
w0 Solitary frequency
0.18
0.16
0.14
0.12
0.1
0.08
0.06
0.04
0.02
0
-1
-0.8
-0.6
-0.4
-0.2
0
0.2
0.4
0.6
0.8
1

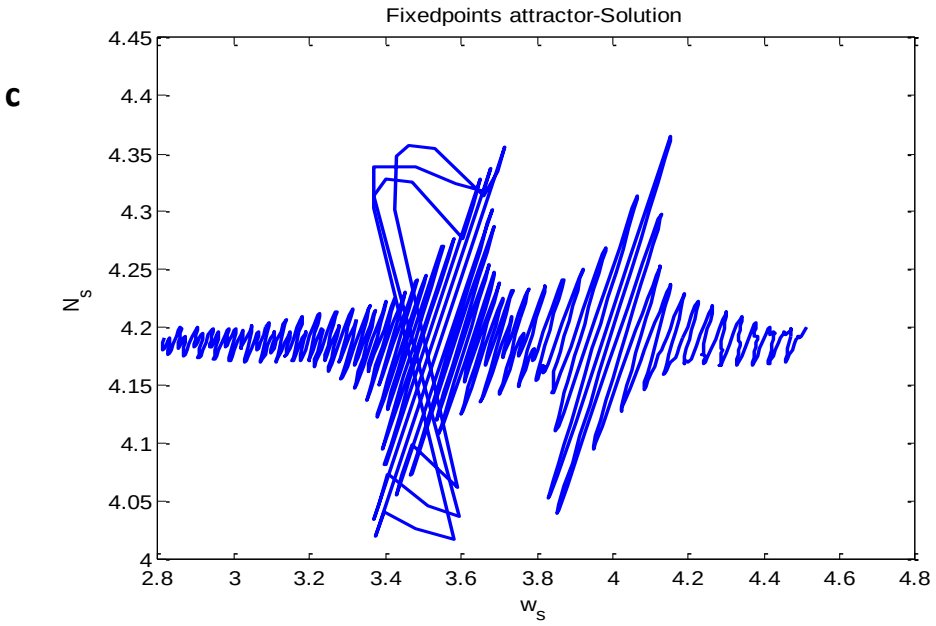

Fig.5: (a) (Ω_S, Ω_o) plane explained the fixed points on it at k_1 =k_2=0.25, $\tau_1 = 3.8$, $\tau_2 = 8$ and $\omega_{f1} = 50/pi$, $\omega_{f2} = -2.5/pi$. (b) in (C_{eff}, Ω_o) plane projected the EFMs branches on it. The first and second filters are represented by blue and red curves respectively. With the appearance of the solitary QD-laser frequency is changed, the fixed points are established and ruined in CW-state bifurcations. (c) EFMs branches predictably addicted to the (N_S, ω_s) plane.

EFMs of DFOF under the influence of changing(k_1 *and* k_2)

The feedback phase difference is introduced as a regular parameter that controls the feedback strength arising from interference between the two filter fields to achieve a non-trivial reduction from the DFOF laser to the single FOF laser. When a large value is taken for k_1, such as 0.4, this value has a clear effect, as we notice the clarity and largeness of the Lorentz profile for the first filter, as this region extends from 3.7 to 4.3, as shown in Fig. 6(a).

Fig. 6(b) shows us a clear rise in the pulse of the first filter, with a distortion at its peak, where its height reaches 0.255. This height is very large compared to the pulse of the second filter, where its height reaches 0.15. We also note that the wiggling shape of the first filter is large compared to the second filter, in addition to the appearance of a saddle node Large, as shown in Fig. 6(c).

When the value of k_2 is increased, this increase leads to the Lorentz region of the second filter becoming larger, with its vanishing at the edges, where the region extends from 3.1 to 3.9, and this region is much larger than what we obtained in the case of the single filter, as shown in Fig. 7(a). Fig. 7(b) shows us a significant increase in the pulse of the second filter, as this increase is accompanied by a distortion of the peak of the pulse, and the pulse height reaches 0.35, while the pulse of the first filter reaches 0.15. The filter width and feedback intensity affect the saddle-node behaviour in the wiggly form because they can be increased to produce MMO behavior as seen in Fig. 7(c).

a

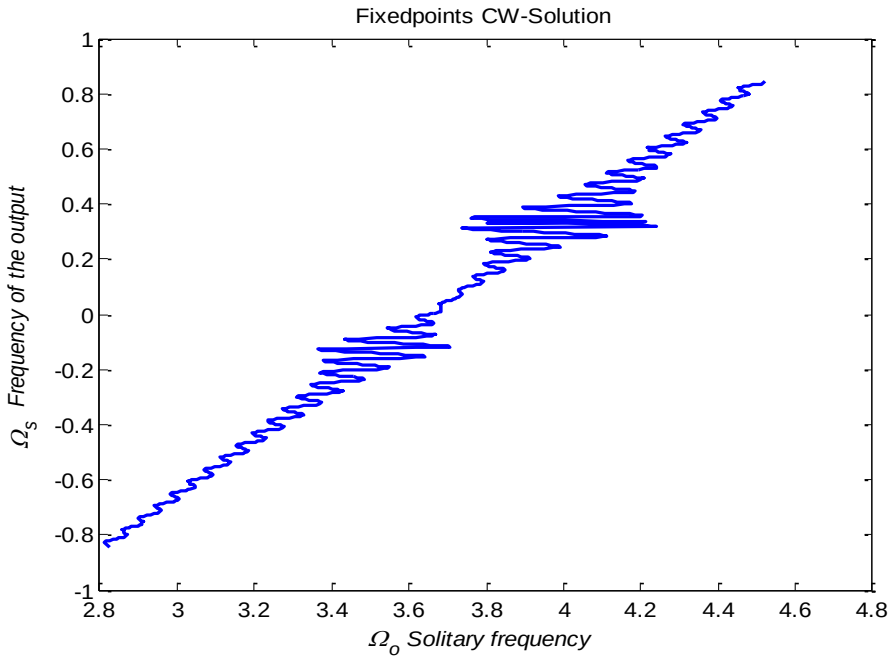
Fixedpoints CW-Solution
Ωs Frequency of the output
Ωo Solitary frequency
1
0.8
0.6
0.4
0.2
0
-0.2
-0.4
-0.6
-0.8
-1
2.8
3
3.2
3.4
3.6
3.8
4
4.2
4.4
4.6
4.8

b

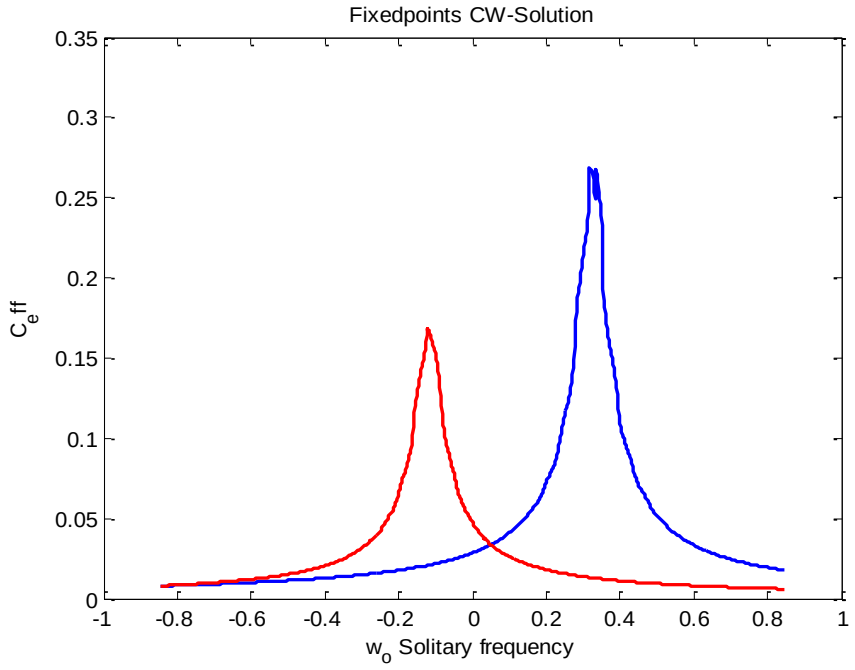
Fixedpoints CW-Solution
Ce ff
wo Solitary frequency
0.35
0.3
0.25
0.2
0.15
0.1
0.05
0
-1
-0.8
-0.6
-0.4
-0.2
0
0.2
0.4
0.6
0.8
1

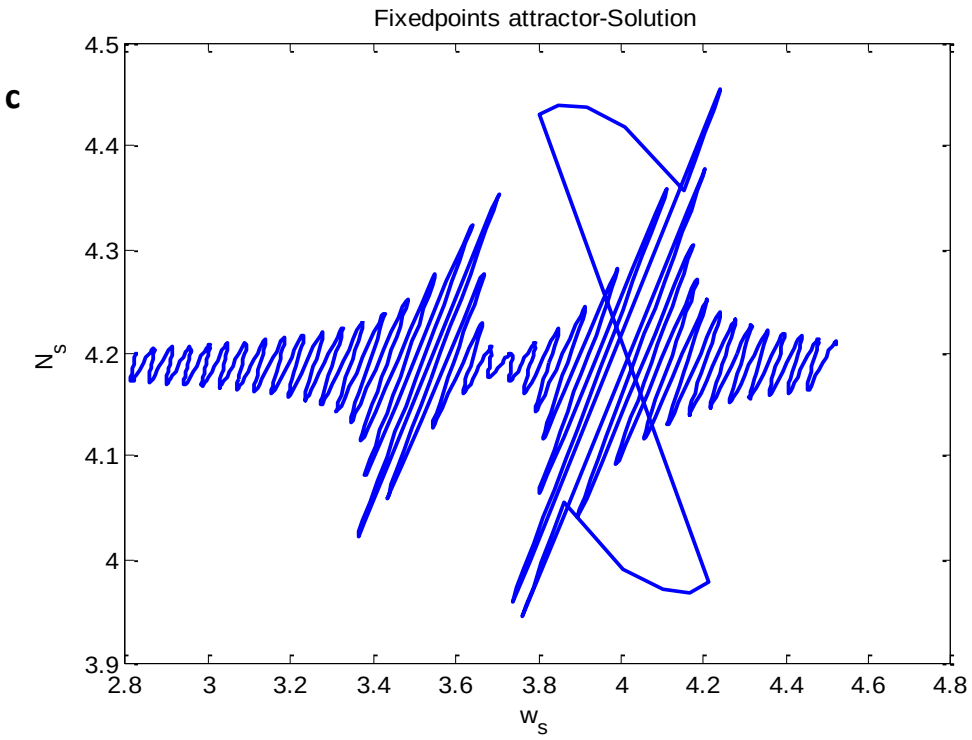

Fig.6: (a) (Ω_S, Ω_o) plane explained the fixed points on it at $k_1 = 0.4$, =k_2=0.25, $\tau_1 = 3.8$, $\tau_2 = 3.8$ and $\omega_{f1} = 50/pi$, $\omega_{f2} = -2.5/pi$. (b) in (C_{eff}, Ω_o) plane projected the EFMs branches on it. The first and second filters are represented by blue and red curves respectively. With the appearance of the solitary QD-laser frequency is changed, the fixed points are established and ruined in CW-state bifurcations. (c) EFMs branches predictably addicted to the (N_S, ω_s) plane.

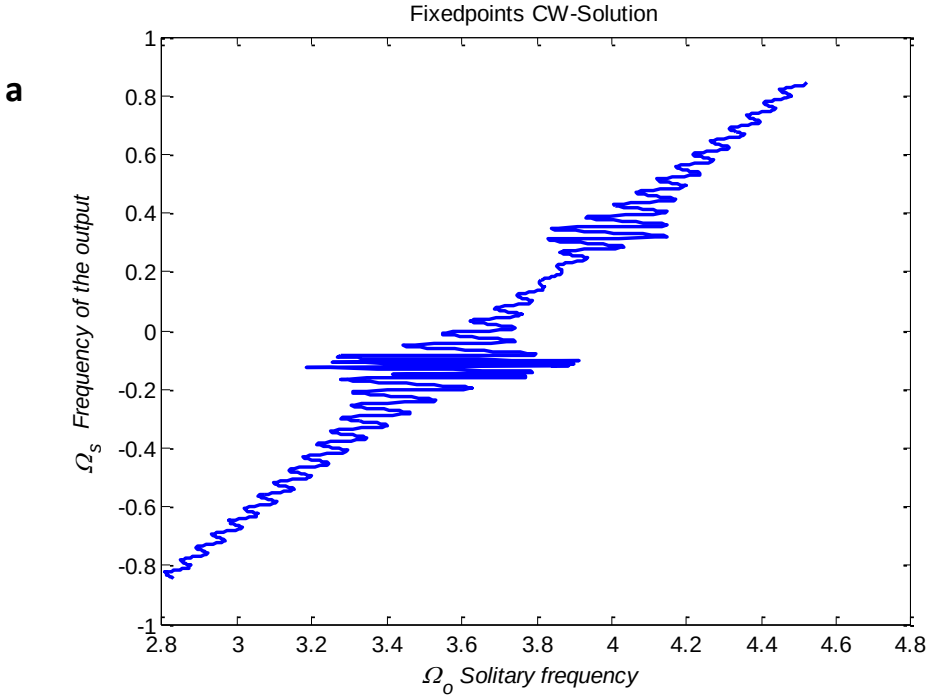

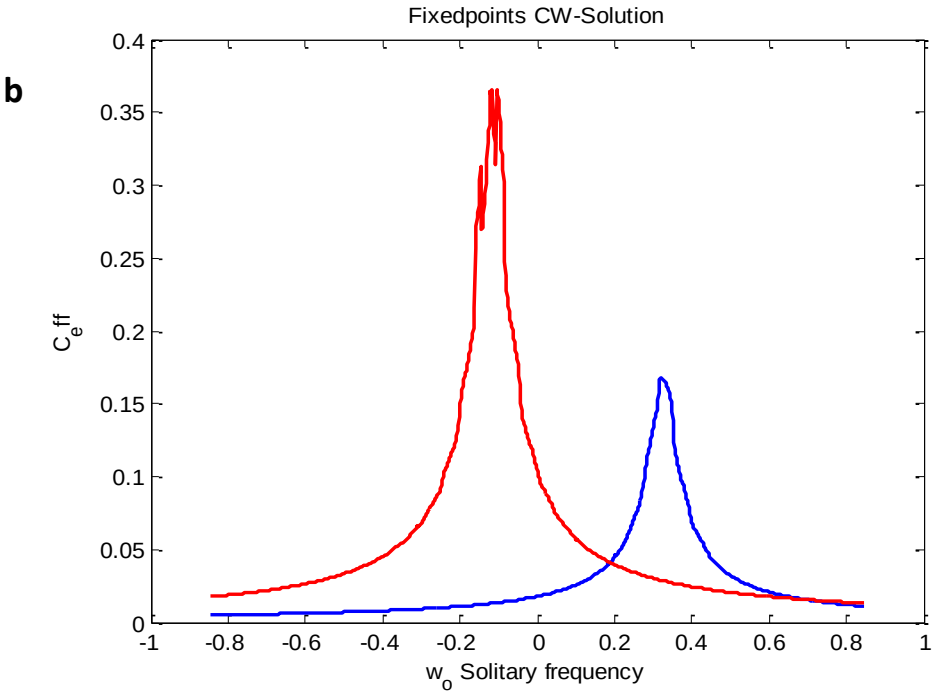

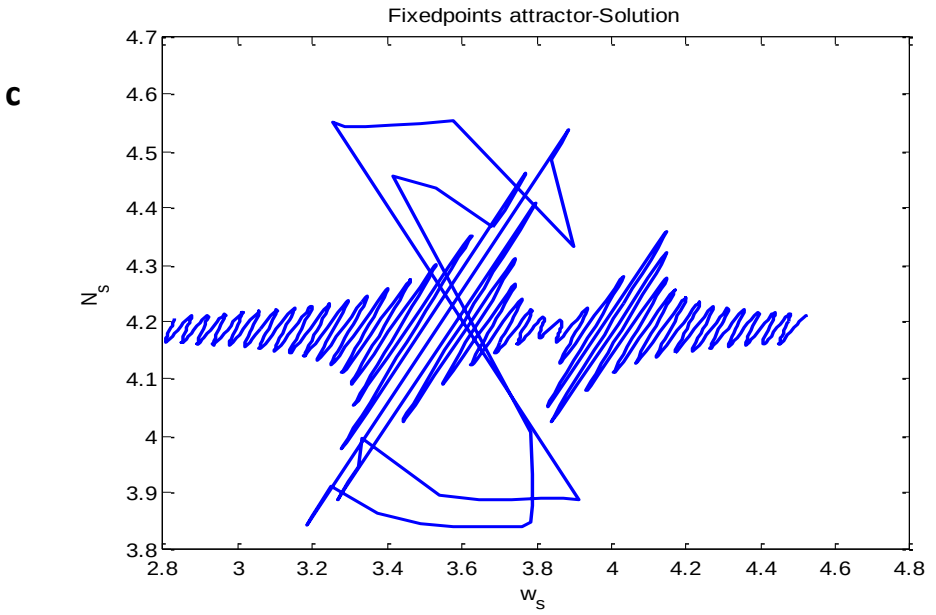

Fig.7: (a) (Ω_S, Ω_o) plane explained the fixed points on it at $k_1 = 0.25$, =k_2=0.55, $\tau_1 = 3.8$, $\tau_2 = 3.8$ and $\omega_{f1} = 50/pi$, $\omega_{f2} = -2.5/pi$. (b) in (C_{eff}, Ω_o) plane projected the EFMs branches on it. The first and second filters are represented by blue and red curves respectively. With the appearance of the solitary QD-laser frequency is changed, the fixed points are established and ruined in CW-state bifurcations. (c) EFMs branches predictably addicted to the (N_S, ω_s) plane.

CONCLUSION

In our current work, we present a study of the EFM structure of a DFOF laser. The focus of this work is on the relationship between the surface EFM and key parameters, such as the two detuning ω_{f1} and ω_{f2}, the feedback strength k_1 and k_2, and the delay time τ_1 andτ_2 of two filters. We have taken large and small values for each of the above parameters. We got the highest pulse peak when we fixed k_1 and changed k_2 from 0.25 to 0.55, since the 3545

pulse peak of the second filter reached 0.35 and the filter width and feedback intensity affect the saddle-node behavior in the wiggly form because they can be increased to produce MMO behavior. On the EFM surface, we discovered that there are regions of stable EFMs that are bordered by saddle-node and Hopf bifurcations. Understanding how the stability areas change by adjustments of the numerous system characteristics is a major challenge.

REFERENCES

[1] R. Broom, "Self modulation at gigahertz frequencies of a diode laser coupled to an external cavity," *Electronics Letters,* vol. 23, no. 5, pp. 571-572, 1969.

[2] R. Broom, E. Mohn, C. Risch, and R. Salathe, "Microwave self-modulation of a diode laser coupled to an external cavity," *IEEE Journal of Quantum Electronics,* vol. 6, no. 6, pp. 328-334, 1970.

[3] X. Porte, D. Brunner, I. Fischer, and M. C. Soriano, "Nonlinear Dynamics of a Single-Mode Semiconductor Laser with Long Delayed Optical Feedback: A Modern Experimental Characterization Approach," in *Photonics*, 2022, vol. 9, no. 1: MDPI, p. 47.

[4] M. Yousefi, D. Lenstra, G. Vemuri, and A. Fischer, "Control of nonlinear dynamics of a semiconductor laser with filtered optical feedback," *IEE PROCEEDINGS OPTOELECTRONICS,* vol. 148, no. 5/6, pp. 233-237, 2001.

[5] G. Van Tartwijk and D. Lenstra, "Semiconductor lasers with optical injection and feedback," *Quantum and Semiclassical Optics: Journal of the European Optical Society Part B,* vol. 7, no. 2, p. 87, 1995.

[6] O. K. Andersen, A. P. Fischer, I. C. Lane, E. Louvergneaux, S. Stolte, and D. Lenstra, "Experimental stability diagram of a diode laser subject to weak phase-conjugate feedback from a rubidium vapor cell," *IEEE journal of quantum electronics,* vol. 35, no. 4, pp. 577-582, 1999.

[7] A. Fischer, M. Yousefi, D. Lenstra, M. W. Carter, and G. Vemuri, "Experimental and theoretical study of semiconductor laser dynamics due to filtered optical feedback," *IEEE Journal of selected topics in quantum electronics,* vol. 10, no. 5, pp. 944-954, 2004.

[8] M. Yousefi, A. P. Fischer, D. Lenstra, M. W. Carter, and G. Vemuri, "Dynamics in the Frequency of a Semiconductor Laser using Feedback from a Narrow Filter," in *8th Annual Symposium of the IEEE/LEOS Benelux Chapter, November 20-21, 2003, Enschede, Netherlands*, 2003: Institute of Electrical and Electronics Engineers, pp. 13-16.

[9] D. O'Brien, S. Hegarty, G. Huyet, and A. Uskov, "Sensitivity of quantum-dot semiconductor lasers to optical feedback," *Optics letters,* vol. 29, no. 10, pp. 1072-1074, 2004.

[10] T. Simpson, J.-M. Liu, A. Gavrielides, V. Kovanis, and P. Alsing, "Period-doubling cascades and chaos in a semiconductor laser with optical injection," *Physical review A,* vol. 51, no. 5, p. 4181, 1995.

[11] A. Karim, "Frustrated instabilities and chaos in semiconductor laser amplifiers," *PROCEEDINGS OF THE ROMANIAN ACADEMY SERIES A-MATHEMATICS PHYSICS TECHNICAL SCIENCES INFORMATION SCIENCE,* vol. 9, no. 2, pp. 99-103, 2008.

[12] J. Mørk, J. Mark, and B. Tromborg, "Route to chaos and competition between relaxation oscillations for a semiconductor laser with optical feedback," *Physical review letters,* vol. 65, no. 16, p. 1999, 1990.

[13] H. Erzgräber, B. Krauskopf, D. Lenstra, A. Fischer, and G. Vemuri, "Frequency versus relaxation oscillations in a semiconductor laser with coherent filtered optical feedback," *Physical Review E,* vol. 73, no. 5, p. 055201, 2006.

[14] B. Haegeman, K. Engelborghs, D. Roose, D. Pieroux, and T. Erneux, "Stability and rupture of bifurcation bridges in semiconductor lasers subject to optical feedback," *Physical Review E,* vol. 66, no. 4, p. 046216, 2002.

[15] T. Heil, I. Fischer, W. Elsäßer, B. Krauskopf, K. Green, and A. Gavrielides, "Delay dynamics of semiconductor lasers with short external cavities: Bifurcation scenarios and mechanisms," *Physical Review E,* vol. 67, no. 6, p. 066214, 2003.

[16] S. M. V. Lunel and B. Krauskopf, "The mathematics of delay equations with an application to the Lang-Kobayashi equations," in *AIP Conference Proceedings*, 2000, vol. 548, no. 1: American Institute of Physics, pp. 66-86.

[17] H. B. Al Husseini and K. A. Al Naimee, "Different Approaches of Synchronization in Chaotic-Coupled QD Lasers," *Chaos Theory,* 2018.

[18] Y. Liu, H. Chen, J. Liu, P. Davis, and T. Aida, "Synchronization of optical-feedback-induced chaos in semiconductor lasers by optical injection," *Physical Review A,* vol. 63, no. 3, p. 031802, 2001.

[19] H. Erzgräber, D. Lenstra, B. Krauskopf, A. Fischer, and G. Vemuri, "Feedback phase sensitivity of a semiconductor laser subject to filtered optical feedback: Experiment and theory," *Physical Review E,* vol. 76, no. 2, p. 026212, 2007.

[20] P. Slowiński, B. Krauskopf, and S. Wieczorek, "Solution structure and dynamics of a semiconductor laser subject to feedback from two external filters," in *Semiconductor Lasers and Laser Dynamics IV*, 2010, vol. 7720: SPIE, pp. 126-136.

[21] A. S. Mahdi and H. B. Al Husseini, "Filtered optical feedback modes effect on quantum-dot laser behavior," *Journal of Optics,* pp. 1-12, 2023.

[22] K. Green and B. Krauskopf, "Mode structure of a semiconductor laser subject to filtered optical feedback," *Optics communications,* vol. 258, no. 2, pp. 243-255, 2006.

DOI: https://doi.org/10.15379/ijmst.v10i3.3396